Dinuclear Nickel(II) Complexes of an Unsymmetric "End-Off" Compartmental Ligand: Conversion of Urea into Cyanate at a Dinuclear Nickel Core

Syunsuke Uozumi,[†] Hideki Furutachi,[†] Masaaki Ohba,[†] Hisashi Ōkawa,*[,†] David E. Fenton,[‡] Kenji Shindo,[§] Susumu Murata,[§] and David J. Kitko[§,||]

Department of Chemistry, Faculty of Science, Kyushu University, Hakozaki, Higashiku, Fukuoka 812-8581, Japan, Department of Chemistry, The University of Sheffield, Sheffield S3 7HF, U.K., and Procter and Gamble Far East Inc., Koyo-cho, Naka 1-17, Higashinada-ku, Kobe 658-0032, Japan

Received July 7, 1998

A phenol-based "end-off" compartmental ligand, 2-[*N*,*N*-di(2-pyridylmethyl)aminomethyl]-6-{*N*-[2-(dimethylamino)ethyl]iminomethyl}-4-methylphenol (HL), having an iminic bidentate and an aminic tridentate chelating arms on the 2- and 6-positions of the phenolic ring, respectively, forms dinuclear nickel complexes $[Ni_2(L)(AcO)(NCS)_2]$ (**1**), $[Ni_2(L)(AcO)_2(MeOH)]PF_6$ (**2**), and $[\{Ni_2(L)(OH)(MeOH)\}_2(CO_3)](PF_6)_2$ (**3**). Complex **1** crystallizes in the monoclinic space group $P2_1/c$, $a = 14.165(5)$ Å, b=15.198(4) Å, $c = 17.395(8)$ Å, $\beta = 100.62(4)°$, $V = 3680(2)$ Å^3, and $Z = 4$. The pair of Ni ions present are bridged by the phenolic oxygen of L^- and an acetate group in *syn*−*syn* mode (Ni−Ni: 3.373(3) Å). An isothiocyanate nitrogen atom coordinates to each Ni providing an asymmetric dinuclear core with a mixed {5/6} coordination number set. Complex **2** crystallizes in the monoclinic space group $P2_1/c$, $a = 13.505(5)$ Å, $b = 12.028(4)$ Å, $c = 22.774(9)$ Å, $\beta = 103.78(3)°$, $V = 3592(2)$ Å^3, and $Z = 4$. It has a dinuclear core bridged by the phenolic oxygen of L^- and two acetate groups in *syn*−*syn* mode, providing a μ-phenoxo-bis(μ-carboxylato)dinickel(II) core (Ni−Ni: 3.396(6) Å). A methanol molecule coordinates to the Ni bound to the bidentate arm, forming a dinuclear core having a {6/6} coordination number set and an asymmetric donor atom environment. Complex **3** crystallizes in the orthorhombic space group *Pbcn*, $a = 19.056(5)$ Å, $b = 18.997(4)$ Å, $c = 19.919(6)$ Å, $\alpha = \beta = \gamma = 90°$, $V = 7211(5)$ Å^3, and $Z = 8$. In each dinuclear unit a pair of Ni ions are bridged by the phenolic oxygen of L^- and a hydroxo oxygen (Ni−Ni: 3.087(2) Å). A carbonate further bridges two of the dinuclear units to present a composite dimer. The Ni bound to the bidentate arm attains six-coordinate geometry by further interaction with two oxygens of the bridging carbonato group. The Ni bound to the tridentate arm assumes six-coordinate geometry by further coordination of a methanol oxygen. Complexes **1**−**3** react with urea in ethanol to form the isocyanate complexes $[Ni_2(L)(AcO)(NCS)(NCO)]$ (**1′**), $[Ni_2(L)(AcO)(NCO)(EtOH)]PF_6$ (**2′**), and $[\{Ni_2(L)(NCO)(EtOH)\}_2(CO_3)](PF_6)_2$ (**3′**), respectively. Complex **3′** crystallizes in the triclinic space group $P\bar{1}$, $a = 20.072(7)$ Å, $b = 21.145(6)$ Å, $c = 18.688(6)$ Å, $\alpha = 106.20(2)°$, $\beta = 90.01(3)°$, $\gamma = 88.73(3)°$, $V = 7614(4)$ Å^3, and $Z = 4$. It has a dimeric structure very similar to that of **3**, except for the replacement of the hydroxy bridge and the methanol ligand in **3** by isocyanate bridge and ethanol ligand, respectively, in **3′**.

Introduction

Bimetallic cores exhibit versatile roles at the active sites of bimetalloenzymes[1] and model studies using simple dinuclear metal complexes is important in order to gain an insight into the biological functions of such bimetallic cores. Recent X-ray crystallographic studies have indicated that most bimetallic biosites are unsymmetric with respect to the donor atoms about two metal centers (donor asymmetry),[2,3] the geometric arrangement of the donor atoms (geometry asymmetry),[4] the coordination number (coordination number asymmetry),[5−7] and/or the nature of the metal ions (metal asymmetry).[8−10] It is considered that biological systems employ such an unsymmetric dinuclear core to achieve specific functions by the conjunction of distinct roles of two metal ions. Thus, the design of compartmental ligands capable of providing an asymmetric dinuclear core is becoming increasingly important.[11]

* Corresponding author. E-mail: okawascc@mbox.nc.kyushu-u.ac.jp.
† Kyushu University.
‡ The University of Sheffield.
§ Procter & Gamble Far East Inc.
|| Present address: The Procter & Gamble Manufacturing Co. Miami Valley Laboratories, 11810 E. Miami River Road, Cincinnati, OH 45061.

(1) Fenton, D. E.; Okawa, H. *Perspectives on Bioinorganic Chemistry*; Hay, R. W., Dilworth, J. R., Nolan, K. B., Eds.; JAI Press: London, 1993; Vol. 2, p 81.
(2) Roderick, S. L.; Matthews, B. W. *Biochemistry* **1993**, *32*, 3907.
(3) Carroll, H. L.; Glusker, J. P.; Birger, V.; Manfre, F.; Tritseh, D.; Bieuman, J. F. *Proc. Natl. Acad. Sci. U.S.A.* **1989**, *86*, 4440.
(4) Nordlund, P.; Sjöberg, B.-M.; Eklund, H. *Nature* **1990**, *345*, 593.
(5) Holmes, M. A.; Le Trong, I.; Turley, S.; Sleker, L. C.; Stenkamp, R. E. *J. Mol. Biol.* **1991**, *218*, 583.
(6) Burley, S. K.; David, P. R.; Taylor, A.; Lipscomb, W. N. *Proc. Natl. Acad. Sci. U.S.A.* **1990**, *87*, 6878.
(7) Jabri, E.; Carr, M. B.; Hausinger, R. P.; Karplus, P. A. *Science* **1995**, *268*, 998.
(8) Sträter, N.; Klabunde, T.; Tucker, P.; Witzel, H.; Krebs, B. *Science* **1995**, *268*, 1489.
(9) Kissinger, C. R.; Parge, H. E.; Knighton, D. R.; Llewis, C. T.; Pelletier, L. A.; Tempczyk, A.; Kalish, V. J.; Tucker, K. D.; Showalter, R. E.; Moomaw, E. W.; Gastinel, L. N.; Habuka, N.; Chen, X. Y.; Maldonado, F.; Barker, J. E.; Bayquet, R.; Villafranca, J. E. *Nature* **1995**, *378*, 641.
(10) Egloff, M.-P.; Cohen, P. T. W.; Reinemer, P.; Barford, D. *J. Mol. Biol.* **1995**, *254*, 942.
(11) Fenton, D. E.; Okawa, H. *Chem. Ber.* **1997**, **130**, 433.

10.1021/ic9807689 CCC: $15.00
Published on Web 11/11/1998

Chart 1. Chemical Structure of HL

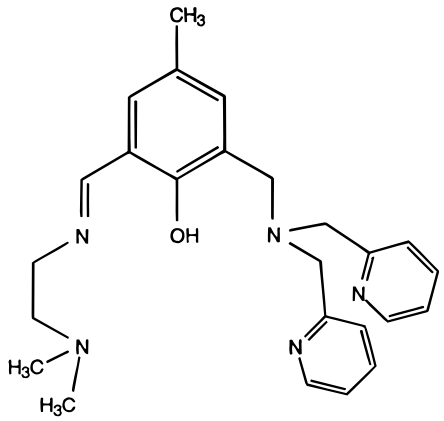

Phenol-based compartmental ligands of the "end-off" type, possesssing two chelating arms attached to the 2- and 6-positions of the phenol ring, have been used to provide dinuclear metal complexes bridged by the endogenous phenolic oxygen and one or two exogenous groups. It has been shown that μ-phenoxobis(μ-carboxylato)dimanganese(II) core complexes derived from such ligands are good functional models of manganese catalase.[12−16] Analogous ligands having two tridentate chelating arms have been used by Suzuki[17] for modeling nonheme bimetallic biosites.

In this study a new phenol-based end-off compartmental ligand, 2-[*N*,*N*-di(2-pyridylmethyl)aminomethyl]-6-{*N*-[2-(dimethylamino)ethyl]iminomethyl}-4-methylphenol (abbreviated as HL, see Chart 1), has been prepared. It has iminic bidentate and aminic tridentate chelating arms attached to the 2- and 6-positions of the phenol ring, and in our preliminary study[18] it formed a dinuclear copper(II) complex that is geometrically asymmetric with respect to the two Cu^{II} ions. Our present purpose using HL is to provide a model for the active site of urease, a metalloenzyme employing a dinuclear nickel core having a coordination number asymmetry to hydrolyze urea into ammonia and carbon dioxide.[7,19,20] Three dinuclear nickel complexes have been derived: $[Ni_2(L)(AcO)(NCS)_2]$ (**1**), $[Ni_2(L)(AcO)_2(MeOH)]PF_6$ (**2**), and $[\{Ni_2(L)(OH)(MeOH)\}_2(CO_3)](PF_6)_2$ (**3**). X-ray crystallographic studies have demonstrated the presence of an asymmetric dinuclear core for **1** and **2** and a carbonato-bridged dimeric structure of an asymmetric dinuclear core for **3**. Emphasis is placed on the reaction of **1**−**3** with urea to form the isocyanate complexes $[Ni_2(L)(AcO)(NCS)(NCO)]$ (**1′**), $[Ni_2(L)(AcO)(NCO)(EtOH)]PF_6$ (**2′**), and $[\{Ni_2(L)(NCO)(EtOH)\}_2(CO_3)](PF_6)_2$ (**3′**).

Experimental Section

Measurements. Elemental analyses of C, H, and N were obtained from the Service Center of Elemental Analysis at Kyushu University. Analyses of nickel were obtained using a Shimadzu AA-660 atomic absorption/flame emission spectrophotometer. Infrared spectra were recorded on a JASCO IR-810 spectrometer using KBr disks. FAB mass spectra were recorded on a JMS-SX/SX102A tandem mass spectrometer by the use of *m*-nitrobenzyl alcohol or 2-nitrophenyl octyl ether as the matrix. Electronic spectra were measured in *N*,*N*-dimethylformamide (DMF) using a Shimadzu UV-3100PC spectrometer. Magnetic susceptibilities were determined on a Faraday balance in the temperature range of 78−300 K. Effective magnetic moments were calculated by the equation $\mu_{eff} = 2.828(\chi_A T)^{1/2}$, where χ_A is the magnetic susceptibility per nickel corrected for diamagnetism of the constituting atoms.

Preparations. 5-Methylsalicylaldehyde was synthesized by the Duff reaction.[21] 3-Chloromethyl-5-methylsalicylaldehyde was prepared by a modification of the literature method.[22] Other chemicals were purchased from commercial sources.

3-[*N*,*N*-Di(2-pyridylmethyl)aminomethyl]-5-methylsalicylaldehyde (HL′). A solution of di(2-pyridylmethyl)amine (9.9 g, 100 mmol) in tetrahydrofuran (15 cm^3) was dropwise added to a stirred solution of 3-chloromethyl-5-methylsalicylaldehyde (9.2 g, 50 mmol) in tetrahydrofuran (30 cm^3) at 0 °C, and the mixture was stirred at this temperature for 2 h. Di(2-pyridylmethyl)amine hydrochloride that precipitated was separated by filtration, and the filtrate was evaporated to dryness. The residue was dissolved in dichloromethane (50 cm^3), and the solution was shaken with three 50 cm^3 portions of 10% KOH solution. The aqueous layers were combined and neutralized with 6% hydrochloric acid. The resulting turbid solution was shaken with three 50 cm^3 portions of dichloromethane and the combined extract was evaporated to dryness. The crude product was crystallized from methanol as yellow microcrystals. Yield: 8.827 g (51.0%). It melted at 135 °C. Selected IR data (ν/cm^{-1}) using KBr disk: 3040, 2850, 1680, 1610, 1590, 1560, 1480, 1470, 1440, 1390, 1380, 1300, 1280, 1230, 1210, 1150, 1110, 1000, 860, 770. ^{1}H NMR [δ/ppm in $CDCl_3$]: 11.72 (s, 1H, OH); 10.43 (s, 1H, CHO); 8.58, 7.65, 7.44, and 7.21 (8H, pyridine H); 7.40, 7.37, and 7.21 (2H, aromatic H); 3.89 (s, 4H, N-CH_2-py); 3.80 (s, 2H, Ar-CH_2-N); 2.27 (s, 3H, Me).

$[Ni_2(L)(AcO)(NCS)_2]$ (1). The ligand HL was prepared in situ by reacting HL′ (0.174 g, 0.5 mmol) and *N*,*N*-dimethylethylenediamine (0.044 g, 0.5 mmol) in methanol (5 cm^3) at the reflux temperature. To the resulting yellow solution was added nickel(II) acetate tetrahydrate (0.249 g, 1.0 mmol), and the mixture was refluxed for 30 min. The addition of sodium thiocyanate (0.081 g, 1.0 mmol) resulted in the precipitation of green microcrystals. Yield: 0.199 g (56%). Selected IR data (ν/cm^{-1}) using KBr disk: 3450, 3000−2800, 2100, 2060, 1640, 1600,1560, 1460, 1440, 1300, 1020, 760. UV−vis [λ/nm (ϵ/M^{-1} cm^{-1}) in DMF: 366 (3800), 595 (27), 765 (17), 954 (40).

$[Ni_2(L)(AcO)_2(MeOH)]PF_6$ (2). This complex was obtained as green microcrystals by a method similar to that of **1** using ammonium hexafluorophosphate (0.082 g, 0.5 mmol) instead of sodium thiocyanate. Yield: 0.257 g (62%). Selected IR data (ν/cm^{-1}) using KBr disk: 3400, 3000−2800, 1640, 1605, 1580, 1560, 1460, 1440, 1300, 1020, 840, 770, 560. Molar conductance (Λ_M/S cm^2 mol^{-1}) in DMF: 93. UV−vis [λ/nm (ϵ/M^{-1} cm^{-1}) in DMF: 364 (4400), 604 (30), 767 (15), 954 (43).

$[\{Ni_2(L)(OH)(MeOH)\}_2(CO_3)](PF_6)_2$ (3). The ligand HL was prepared by the reaction of HL′ (0.174 g, 0.5 mmol) and *N*,*N*-dimethylethylenediamine (0.044 g, 0.5 mmol) in methanol (5 cm^3). To this solution were added a methanolic solution of nickel(II) perchlorate hexahydrate (0.366 g, 1.0 mmol) and a methanolic solution of potassium hexafluorophosphate (0.368 g, 2.0 mmol). The mixture was once filtered to separate any insoluble material and refluxed for 30 min to give a green precipitate. Yield: 0.415 g (57%). Selected IR data (ν/cm^{-1}) using KBr disk: 3630, 3400, 3000−2800, 1640, 1600, 1560, 1460, 1300, 1020, 840, 760, 550. Molar conductance (Λ_M/S cm^2 mol^{-1}) in DMF: 112. UV−vis [λ/nm (ϵ/M^{-1} cm^{-1}) in DMF: 364 (4400), 652 (24), 781 (14), 1017 (29).

Reaction of 1−3 with Urea. To a solution of a dinickel complex (2.5×10^{-4} mmol) in ethanol (20 cm^3) was added powdered urea (large excess), and the mixture was stirred at the reflux temperature for 12 h.

(12) Sakiyama, H.; Ōkawa, H.; Isobe, R. *J. Chem. Soc., Chem. Commun.* **1993**, 882.
(13) Sakiyama, H.; Tamaki, H.; Kodera, M.; Matsumoto, N.; Ōkawa, H. *J. Chem. Soc., Dalton Trans.* **1993**, 591.
(14) Sakiyama, H.; Ōkawa, H.; Suzuki, M. *J. Chem. Soc., Dalton Trans.* **1993**, 3832.
(15) Higuchi, C.; Sakiyama, H.; Ōkawa, H.; Isobe, R.; Fenton, D. E. *J. Chem. Soc., Dalton Trans.* **1994**, 1097.
(16) Higuchi, C.; Sakiyama, H.; Ōkawa, H.; Fenton, D. E. *J. Chem. Soc., Dalton Trans.* **1995**, 4015.
(17) Ohkubo, T.; Sugimoto, H.; Nagayama, T.; Masuda, H.; Sato, T.; Tanaka, K.; Maeda, Y.; Ōkawa, H.; Hayashi, Y.; Uehara, A.; Suzuki, M. *J. Am. Chem. Soc.* **1996**, *118*, 701.
(18) Uozumi, S.; Ohba, M.; Ōkawa, H.; Fenton, D. E. *Chem. Lett.* **1997**, 673.
(19) Lippard, S. J. *Science* **1995**, *268*, 996.
(20) Kolodziej, A. F. *Prog. Inorg. Chem.* **1994**, *41*, 493.
(21) Duff, J. C. *J. Chem. Soc.* **1941**, 547.
(22) Lock, G. *Chem. Ber.* **1930**, *63*, 551.

Table 1. Crystal Parameters for $[Ni_2(L)(AcO)(NCS)_2]$ (**1**), $[Ni_2(L)(AcO)_2(MeOH)]PF_6$ (**2**), $[\{Ni_2(L)(OH)(MeOH)\}_2(\mu\text{-}CO_3)](PF_6)_2$ (**3**), and $[\{Ni_2(L)(NCO)(EtOH)\}_2(\mu\text{-}CO_3)](PF_6)_2$ (**3′**)

	1	**2**	**3**	**3′**
formula	$C_{29}H_{33}N_7Ni_2O_3S_2$	$C_{30}H_{40}N_5F_6Ni_2O_6P$	$C_{53}H_{76}N_{10}F_{12}Ni_4O_{12}P_2$	$C_{58}H_{70}N_{12}F_{12}Ni_4O_{10}P_2$
cryst color	green	green	green	green
fw	709.14	829.04	1569.97	1619.99
cryst size/mm^3	0.20 × 0.20 × 0.20	0.20 × 0.20 × 0.20	0.21 × 0.23 × 0.20	0.50 × 0.50 × 0.50
cryst syst	monoclinic	monoclinic	orthorhombic	triclinic
space group	$P2_1/c$	$P2_1/c$	$Pbcn$	$P\bar{1}$
a/Å	14.165(5)	13.505(5)	19.056(5)	20.072(7)
b/Å	15.198(4)	12.028(4)	18.997(4)	21.145(6)
c/Å	17.395(8)	22.774(9)	19.919(6)	18.688(6)
α/deg				106.20(2)
β/deg	100.62(4)	103.78(3)		90.01(3)
γ/deg				88.73(3)
V/Å^3	3680(2)	3592(2)	7211(5)	7614(4)
Z value	4	4	8	4
D_{calc}/g cm^{-3}	1.280	1.516	2.892	1.413
μ(Mo Kα)/cm^{-1}	11.73	11.59	23.26	11.03
no. of reflcns	3290	4589	3180	9505
R^a	0.079	0.063	0.066	0.092
$R_w{}^{b,c}$	0.100	0.068	0.078	0.103

[a] $R = \sum||F_o| - |F_c||/\sum|F_o|$. [b] $R_w = \{\sum[w(|F_o| - |F_c|)^2]/\sum[wF_o^2]\}^{1/2}$. [c] $w = 1/\sigma^2(F_o)$.

Unreacted urea was removed by filtration, and the filtrate was evaporated to dryness to give a green precipitate. It was crystallized from a dichloromethane/ethanol mixture.

$[Ni_2(L)(AcO)(NCS)(NCO)]$ (1′). Green microcrystals. Yield: 0.026 g (15%). Selected IR data (ν/cm^{-1}) using KBr disk: 2180, 2090, 1640, 1600, 1560, 1460, 1440, 1410, 1300, 1020, 760. UV−vis [λ/nm (ϵ/M^{-1} cm^{-1}) in DMF: 362 (4300), 621 (48), 950 (49).

$[Ni_2(L)(AcO)(NCO)(EtOH)]PF_6$ (2′). Green microcrystals. Yield: 0.027 g (13%). Selected IR data (ν/cm^{-1}) using KBr disk: 2180, 1640, 1610, 1590, 1560, 1460, 1440, 1400, 1300, 1020, 840, 780, 760, 560. UV−vis [λ/nm (ϵ/M^{-1} cm^{-1}) in DMF: 362 (4100), 590 (34), 763 (23), 931 (54).

$[\{Ni_2(L)(NCO)(EtOH)\}_2(CO_3)](PF_6)_2$ (3′). Green crystals. Yield: 0.040 g (10%). Selected IR data (ν/cm^{-1}) using KBr disk: 2180, 1640, 1600, 1560, 1510, 1500, 1460, 1440, 1400, 1310, 840, 760, 560. UV−vis [λ/nm (ϵ/M^{-1} cm^{-1}) in DMF: 366 (4700), 656 (25), 762 (21), 957 (38).

The cyanate complexes **1′**−**3′** were also obtained by the reaction of **1**−**3** with potassium cyanate in the 1:1 stoichiometry in boiling ethanol (yield > 45%).

Crystal Structure Analyses. A single crystal of **1** was mounted on a glass fiber and coated with epoxy resin. Each single crystal of **2**, **3**, and **3′** was sealed in a capillary tube together with the mother liquor and used for X-ray structural measurements. Intensities and lattice parameters were obtained on a Rigaku AFC-7R automated four-circle diffractometer, using graphite-monochromated Mo Kα radiation (λ = 0.710 69 Å) and a 12 kW rotating anode generator at 23 ± 1 °C. The cell parameters were determined by 25 reflections. For the intensity data collections, the $\omega-2\theta$ scan mode was used to a maximum 2θ value of 50.0° for **1**, **2**, and **3** and 45.0° for **3′**. The weak reflections ($I < 10.0\sigma(I)$) were rescanned (maximum of 4 scans for **1** and **2** and 5 scans for **3** and **3′**) and the counts were accumulated to ensure good counting statistics. Stationary background counts were recorded on each side of the reflection. The ratio of peak counting time to background counting time was 2:1. The diameter of the incident beam collimator was 1.0 mm, the crystal to detector distance was 235 mm, and the computer controlled detector aperture was set to 9.0 × 13.0 mm (horizontal × vertical). Three standard reflections were monitored every 150 reflections. Over the course of data collection, the standard reflections were monitored and decay corrections were applied by a polynomial correction. A linear correction factor was applied to the data to account for the phenomena. The linear absorption coefficient, μ, for Mo Kα radiation was 11.9 cm^{-1} for **1**, 11.7 cm^{-1} for **2**, 23.3 cm^{-1} for **3**, and 11.0 cm^{-1} for **3′**. An empirical absorption correction based on azimuthal scans of several reflections was applied. The intensity data were corrected for Lorentz and polarization factors.

The structures were solved by direct methods and expanded using Fourier technique. Refinements were carried out by the full-matrix least-squares method, where the function minimized is $\Sigma w(|F_o| - |F_c|)^2$ with the weight, $w = 1/\sigma^2(F_o)$. The non-hydrogen atoms were refined anisotropically. Hydrogen atoms were fixed at the calculated positions and were not refined. Full-matrix least-squares refinements were based on observed reflections with $I > 3.00\sigma(I)$. Crystal data parameters for **1**, **2**, **3**, and **3′** are given in Table 1.

The neutral atom scattering factors were taken from Cromer and Wabar.[23] Anomalous dispersion effects were included in F_{calc}; the values for $\Delta f'$ and $\Delta f''$ were those of Creagh and McAuley.[24] The values for the mass attenuation coefficients were those of Creagh and Hubbel.[25] All calculations were performed using the teXsan crystallographic software package of Molecular Structure Corporation.[26]

Results and Discussion

Preparation. The introduction of a single pendant arm into the 3 position of 5-bromosalicylaldehyde by the Mannich reaction followed by the condensation of the resulting proligand with a primary amine was first reported by Fenton as a facile synthetic method to afford unsymmetric phenol-based end-off ligands having an aminic and an iminic pendant arms at the 2- and 6-positions of phenol ring.[27] In principle this method can be applied to a wide range of end-off compartmental ligands possessing one or two donor groups on the aminic nitrogen. Thus, we attempted to introduce the *N*,*N*-bis(2-pyridylmethyl)-aminomethyl residue into the 3-position of 5-bromosalicylaldehyde by the Mannich reaction, but this resulted in the recovery of the starting materials despite many efforts.

Eventually, the proligand 3-[*N*,*N*-di(2-pyridylmethyl)aminomethyl]-5-methylsalicylaldehyde (HL′) was synthesized in a good yield by the reaction of 3-chloromethyl-5-methylsalicylaldehyde with *N*,*N*-bis(2-pyridylmethyl)amine in 1:2 molar ratio

(23) Cromer, D. T.; Waber, J. T. *International Tables for X-ray Crystallography*; Kynoch Press: Birmingham, 1974; Vol. IV.
(24) Creagh, D. C.; McAuley, W. J. *International Tables for Crystallography*; Wilson, A. J. C., et al., Eds.: Kluwer Academic Publishers: Boston, 1992; pp 219−222.
(25) Creagh, D. C.; Hubbel, J. H. *International Tables for Crystallography*; Wilson, A. J. C., et al., Eds.: Kluwer Academic Publishers: Boston, 1992; pp 200−206.
(26) *TEXSAN*; Molecular Structure Corporation: The Woodlands, TX, 1985.
(27) Crane, J. D.; Fenton, D. E.; Latour, J. M.; Smith A. J. *J. Chem. Soc., Dalton Trans.* **1991**, 2979.

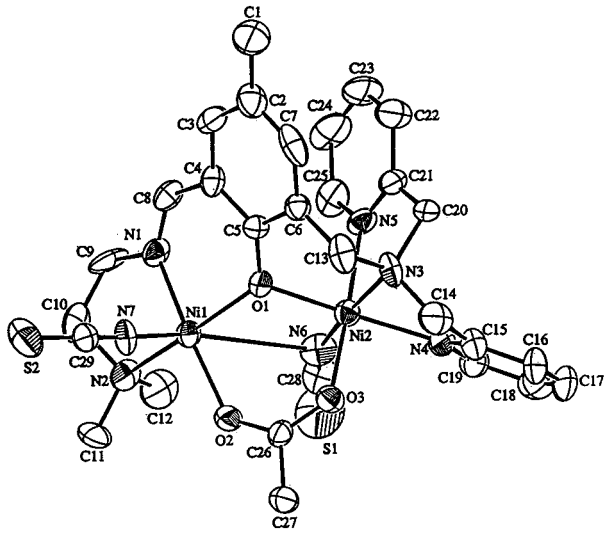

Figure 1. ORTEP view of $[Ni_2(L)(AcO)(NCS)_2]$ (**1**) with the atom numbering scheme.

in tetrahydrofuran. It was characterized by elemental analyses, IR spectra and ^{1}H NMR spectra. The end-off ligand HL was then prepared in situ by the condensation of the proligand with *N*,*N*-dimethylethylenediamine and used for the synthesis of the dinickel complexes **1**−**3**. The reaction of the ligand solution with nickel(II) acetate tetrahydrate in methanol followed by the addition of NaNCS formed $[Ni_2(L)(AcO)(NCS)_2]$ (**1**). A similar reaction using NH_4PF_6 instead of NaNCS gave $[Ni_2(L)(AcO)_2(MeOH)]PF_6$ (**2**). The formation of $[\{Ni_2(L)(OH)(MeOH)\}_2(CO_3)](PF_6)_2$ (**3**) was unexpected. All attempts to obtain a dinickel perchlorate complex by the reaction of HL and nickel(II) perchlorate hexahydrate in methanol were in vain, and addition of a methanolic suspension of KPF_6 to the reaction mixture resulted in the precipitation of **3** after 1 week. The carbonate ion involved certainly originates from interaction of the dinuclear species with atmospheric carbon dioxide. In fact, **3** was not obtained when the synthetic operations were carried out under nitrogen.

Crystal Structures. $[Ni_2(L)(AcO)(NCS)_2]$ (1). An ORTEP[28] view of **1** with the atom numbering scheme is given in Figure 1. Selected bond distances and angles with their estimated standard deviations are listed in Table 2.

The X-ray crystallography has confirmed that a pair of Ni ions are bridged by the phenolic oxygen of L^- and an acetate group in *syn*−*syn* mode with a Ni−Ni intermetallic separation of 3.373(3) Å. An isothiocyanate nitrogen atom binds to each nickel and so the complex has an asymmetric core composed of a {5/6} coordination number set. The geometry about Ni1, bound to the iminic bidentate arm, can be described as a square-pyramid with O1, N1, and N2 of the ligand and O2 of the bridging acetate group on the base and N7 of isocyanate at the apex. The Ni1-donor bond distances fall in the range of 1.977(9)−2.28(1) Å. The geometry about N2, bound to the aminic tridentate arm, is pseudo octahedral. The Ni2-donor bond distances fall in the smaller range of 2.044(9)−2.13(1) Å. The thiocyanate nitrogen N6 is disposed to the open face of the square-pyramidal Ni1 but the Ni1−N6 separation is too long to be considered as a coordination bond (3.28(1) Å). The bridging acetate group coordinates to an equatorial site of Ni1 through O2 but to an axial site of Ni2 through O3 with respect to the mean molecular plane. Because of this the equatorial base of Ni1 is not coplanar with the conjugated part of L^-. This is reflected in the nonplanar configuration at the phenolic oxygen O1; the sum of the bite angles C5−O1−Ni1, C5−O1−Ni2, and Ni1−O1−Ni2 is 356.7°.

(28) Johnson, C. K. Report 3794; Oak Ridge National Laboratory: Oak Ridge, TN, 1965.

Table 2. Selected Bond Distances (Å) and Angles (deg) with Their Estimated Standard Deviations for $[Ni_2(L)(AcO)(NCS)_2]$ (**1**)

Ni(1)−O(1)	1.977(9)	Ni(1)−O(2)	1.982(9)
Ni(1)−N(1)	2.00(1)	Ni(1)−N(2)	2.12(1)
Ni(1)−N(6)	3.28(1)	Ni(1)−N(7)	1.99(1)
Ni(2)−O(1)	2.047(9)	Ni(2)−O(3)	2.044(9)
Ni(2)−N(3)	2.13(1)	Ni(2)−N(4)	2.11(1)
Ni(2)−N(5)	2.05(1)	Ni(2)−N(6)	2.06(1)
O(1)−Ni(1)−O(2)	93.5(4)	O(1)−Ni(1)−N(1)	87.6(4)
O(1)−Ni(1)−N(2)	159.2(5)	O(1)−Ni(1)−N(6)	67.2(4)
O(1)−Ni(1)−N(7)	104.1(4)	O(2)−Ni(1)−N(1)	168.4(5)
O(2)−Ni(1)−N(2)	92.8(4)	O(2)−Ni(1)−N(6)	70.0(4)
O(2)−Ni(1)−N(7)	96.1(5)	N(1)−Ni(1)−N(2)	82.4(5)
N(1)−Ni(1)−N(6)	100.0(4)	N(1)−Ni(1)−N(7)	94.8(5)
N(2)−Ni(1)−N(6)	96.6(5)	N(2)−Ni(1)−N(7)	94.9(5)
N(6)−Ni(1)−N(7)	162.3(4)	O(1)−Ni(2)−O(3)	87.5(4)
O(1)−Ni(2)−N(3)	88.4(4)	O(1)−Ni(2)−N(4)	166.0(4)
O(1)−Ni(2)−N(5)	87.9(4)	O(1)−Ni(2)−N(6)	98.3(5)
O(3)−Ni(2)−N(3)	95.1(4)	O(3)−Ni(2)−N(4)	86.4(4)
O(3)−Ni(2)−N(5)	173.2(4)	O(3)−Ni(2)−N(6)	91.5(5)
N(3)−Ni(2)−N(4)	79.6(5)	N(3)−Ni(2)−N(5)	79.7(5)
N(3)−Ni(2)−N(6)	170.7(5)	N(4)−Ni(2)−N(5)	96.9(4)
N(4)−Ni(2)−N(6)	94.4(5)	N(5)−Ni(2)−N(6)	94.2(5)
Ni(1)−O(1)−Ni(2)	113.9(4)	Ni(1)−N(6)−Ni(2)	74.4(4)

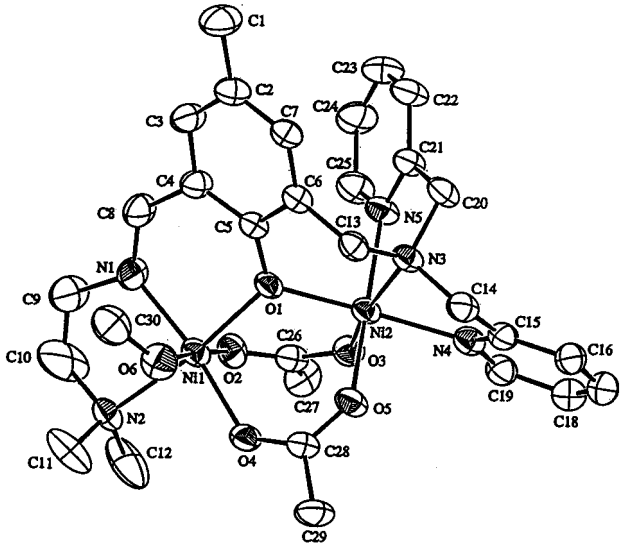

Figure 2. ORTEP view of the $[Ni_2(L)(AcO)_2(MeOH)]^+$ part of **2** with the atom numbering scheme.

$[Ni_2(L)(AcO)_2(MeOH)]PF_6$ (2). A perspective view of **2** with the atom numbering scheme is given in Figure 2. Selected bond distances and angles with their estimated standard deviations are listed in Table 3.

The complex has a dinuclear core bridged by the phenolic oxygen of L^- and two acetate groups in *syn*−*syn* mode, providing a μ-phenoxobis(μ-carboxylato)dinickel(II) core with a Ni−Ni separation of 3.396(6) Å. A methanol molecule coordinates to Ni1, bound to the iminic bidentate arm, forming a donor asymmetric core with a {6/6} coordination number set. The Ni1-donor bond distances fall in the range of 1.98(1)−2.27(1) Å; the Ni1−O6(MeOH) bond (2.27(1) Å) is relatively elongated. The Ni2-donor bond distances fall in the smaller range of 2.01(1)−2.13(1) Å. The Ni1−N1(imine) bond distance (1.99(1) Å) is fairly short relative to the Ni2−N3(amine) distance (2.13(1) Å). The configuration about the phenolic

Table 3. Selected Bond Distances (Å) and Angles (deg) with Their Estimated Standard Deviations for $[Ni_2(L)(AcO)_2(MeOH)]PF_6$ (**2**)

Ni(1)−O(1)	2.018(6)	Ni(1)−O(2)	2.04(1)
Ni(1)−O(4)	1.98(1)	Ni(1)−O(6)	2.27(1)
Ni(1)−N(1)	1.99(1)	Ni(1)−N(2)	2.196(7)
Ni(2)−O(1)	2.033(7)	Ni(2)−O(3)	2.01(1)
Ni(2)−O(5)	2.05(1)	Ni(2)−N(3)	2.13(1)
Ni(2)−N(4)	2.098(9)	Ni(2)−N(5)	2.12(1)
O(1)−Ni(1)−O(2)	93.1(4)	O(1)−Ni(1)−N(4)	95.5(4)
O(1)−Ni(1)−O(6)	87.5(4)	O(1)−Ni(1)−N(1)	89.9(4)
O(1)−Ni(1)−N(2)	172.5(2)	O(2)−Ni(1)−O(4)	96.1(5)
O(2)−Ni(1)−O(6)	175.8(2)	O(2)−Ni(1)−N(1)	92.0(5)
O(2)−Ni(1)−N(2)	87.5(4)	O(4)−Ni(1)−O(6)	79.6(5)
N(1)−Ni(1)−N(1)	169.9(3)	O(4)−Ni(1)−N(2)	91.9(4)
O(6)−Ni(1)−N(1)	92.2(5)	O(6)−Ni(1)−N(2)	92.4(4)
N(1)−Ni(1)−N(2)	82.5(4)	O(1)−Ni(2)−O(3)	100.3(4)
O(1)−Ni(2)−O(5)	87.4(3)	O(1)−Ni(2)−N(3)	91.2(4)
O(1)−Ni(2)−N(4)	168.2(2)	O(1)−Ni(2)−N(5)	90.2(4)
O(3)−Ni(2)−O(5)	96.6(4)	O(3)−Ni(2)−N(3)	165.4(2)
O(3)−Ni(2)−N(4)	89.7(4)	O(3)−Ni(2)−N(5)	90.6(4)
O(5)−Ni(2)−N(3)	92.7(4)	O(5)−Ni(2)−N(4)	85.3(4)
O(5)−Ni(2)−N(5)	172.7(2)	N(3)−Ni(2)−N(4)	79.9(4)
N(3)−Ni(2)−N(5)	80.4(4)	N(4)−Ni(2)−N(5)	96.0(4)
Ni(1)−O(1)−Ni(2)	113.9(4)		

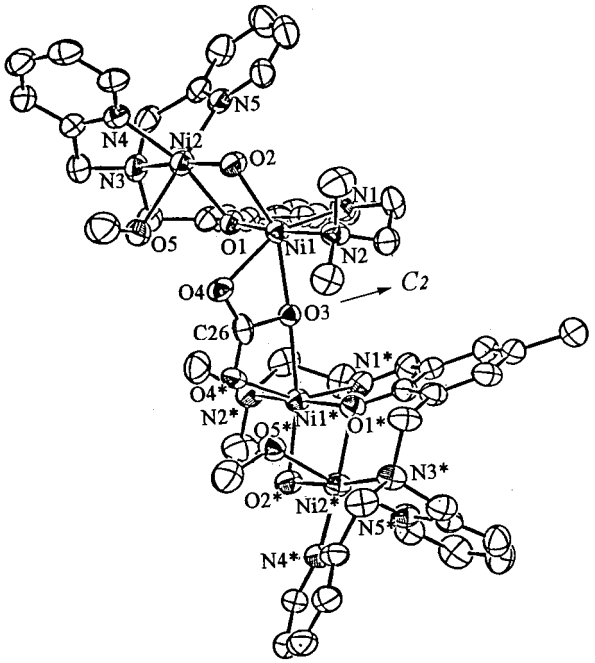

Figure 3. ORTEP view of the $[\{Ni_2(L)(OH)(MeOH)\}_2(CO_3)]^{2+}$ part of **3** with the atom numbering scheme.

oxygen O1 is nearly planar in this complex: the sum of the bite angles of C5−O1−Ni1, C5−O1−Ni2, and Ni1−O1−Ni2 is 359.5°.

$[\{Ni_2(L)(OH)(MeOH)\}_2(CO_3)](PF_6)_2$ (3). A perspective view of **3** with the atom numbering scheme is given in Figure 3. Selected bond distances and angles with their estimated standard deviations are listed in Table 4.

This complex has a carbonato-bridged dimer structure derived from an asymmetric dinuclear unit. The two dinuclear units are correlated by the C_2 axis running along the C26−O3 bond. In each dinuclear unit a pair of Ni ions are bridged by the phenolic oxygen O1 and a hydroxo oxygen O2 with a Ni1−Ni2 intermetallic separation of 3.087(2) Å. The Ni1, bound to the iminic bidentate arm, has six-coordinate geometry composed of the nitrogen donor atoms N1 and N2, the bridging oxygen

Table 4. Selected Bond Distances (Å) and Angles (deg) with Their Estimated Standard Deviations for $[\{Ni_2(L)(OH)(MeOH)\}_2(CO_3)](PF_6)_2$ (**3**)

Ni(1)−O(1)	2.026(7)	Ni(1)−O(2)	2.070(7)
Ni(1)−O(3)	2.155(2)	Ni(1)−O(4)	2.180(8)
Ni(1)−N(1)	2.01(1)	Ni(1)−N(2)	2.15(1)
Ni(2)−O(1)	2.028(7)	Ni(2)−O(2)	2.038(7)
Ni(2)−O(5)	2.188(8)	Ni(2)−N(3)	2.096(9)
Ni(2)−N(4)	2.06(1)	Ni(2)−N(5)	2.07(1)
O(3)−C(26)	1.48(4)	O(4)−C(26)	1.236(9)
O(1)−Ni(1)−O(2)	81.0(3)	O(1)−Ni(1)−O(3)	90.4(2)
O(1)−Ni(1)−O(4)	92.3(3)	O(1)−Ni(1)−N(1)	88.8(4)
O(1)−Ni(1)−N(2)	171.7(4)	O(2)−Ni(1)−O(3)	155.4(8)
O(2)−Ni(1)−O(4)	93.6(3)	O(2)−Ni(1)−N(1)	111.5(4)
O(2)−Ni(1)−N(2)	99.7(3)	O(3)−Ni(1)−O(4)	63.6(9)
O(3)−Ni(1)−N(1)	91.2(9)	O(3)−Ni(1)−N(2)	92.1(3)
O(4)−Ni(1)−N(1)	154.7(3)	O(4)−Ni(1)−N(2)	95.9(4)
N(1)−Ni(1)−N(2)	83.3(4)	O(1)−Ni(2)−O(2)	81.7(3)
O(1)−Ni(2)−O(5)	82.2(3)	O(1)−Ni(2)−N(3)	90.8(3)
O(1)−Ni(2)−N(4)	166.3(4)	O(1)−Ni(2)−N(5)	95.8(3)
O(2)−Ni(2)−O(5)	88.4(3)	O(2)−Ni(2)−N(3)	172.4(3)
O(2)−Ni(2)−N(4)	107.0(4)	O(2)−Ni(2)−N(5)	97.5(4)
O(5)−Ni(2)−N(3)	91.7(4)	O(5)−Ni(2)−N(4)	87.3(4)
O(5)−Ni(2)−N(5)	173.4(4)	N(3)−Ni(2)−N(4)	80.6(4)
N(3)−Ni(2)−N(5)	82.0(4)	N(4)−Ni(2)−N(5)	93.6(4)
Ni(1)−O(1)−Ni(2)	99.2(3)	O(3)−C(26)−O(4)	117(2)
O(3)−C(26)−O(5)	116(2)	O(4)−C(26)−O(5)	127(2)

atoms O1 and O2 and the carbonato oxygens O3 and O4. A significant distortion from regular octahedron is seen owing to the presence of the four-membered chelate ring involving the carbonate ion. The Ni2, bound to the aminic tridentate arm, also assumes a six-coordinate geometry comprised of the nitrogen atoms, the bridging phenoxo oxygen O1, the bridging hydroxo oxygen O2 and the methanol oxygen O5. The Ni2−O5 bond (2.188(8) Å) is significantly elongated relative to other Ni2-donor bonds (2.028(7)−2.096(9) Å). The dimeric structure of this complex is due to bridging by the carbonato group, making bonds to Ni1 through its O3 and O4 atoms and to Ni1* through its O3 and O4* atoms. The Ni1−Ni1* intermetallic separation is 4.308(3) Å.

General Properties. Selected IR spectral data for **1**−**3** are given in the Experimental Section. All the complexes show the ν(C═N) vibration of the azomethine group at ∼1640 cm^{-1}. **1** and **2** show ν_{as}(COO) and ν_s(COO) vibrations of the acetate group at 1560 and 1460 cm^{-1}, respectively. The difference between the two vibration modes is small (<150 cm^{-1}), in accord with the bridging function of the acetate group.[29] The ν(OH) vibration of the hydroxyl group for **3** is seen at 3630 cm^{-1}. **1** shows two ν(CN) vibrations assigned to the isothiocyanate group at 2090 and 2060 cm^{-1} in accord with the presence of two nonequivalent NCS^- groups in the crystal. The corresponding ν(CS) modes are not well resolved owing to the superposition of ligand vibrations. The ν(CO) mode of the carbonate group of **3** may exist around 1560∼1590 cm^{-1},[30] but this band is obscured by ligand vibrations. **1** and **3** show an intense band of hexafluorophosphate ion at 840 cm^{-1}.

The electronic absorption spectra of **1**−**3** in DMF are similar to each other and show an intense band in the near-ultraviolet region and two distinct absorption bands in the visible region (see Experimental Section). The intense band near 365 nm is attributable to the $\pi-\pi^*$ transition band associated with the azomethine linkages.[30,31] The two visible bands are assigned

(29) Deacon, G. B.; Phillips, R. J. *Coord. Chem. Rev.* **1980**, *32*, 227.
(30) Sorrell, T. N.; Allen, W. E.; White, P. S. *Inorg. Chem.* **1995**, *34*, 952.
(31) Bosnich, B. *J. Am. Chem. Soc.* **1968**, *90*, 627.

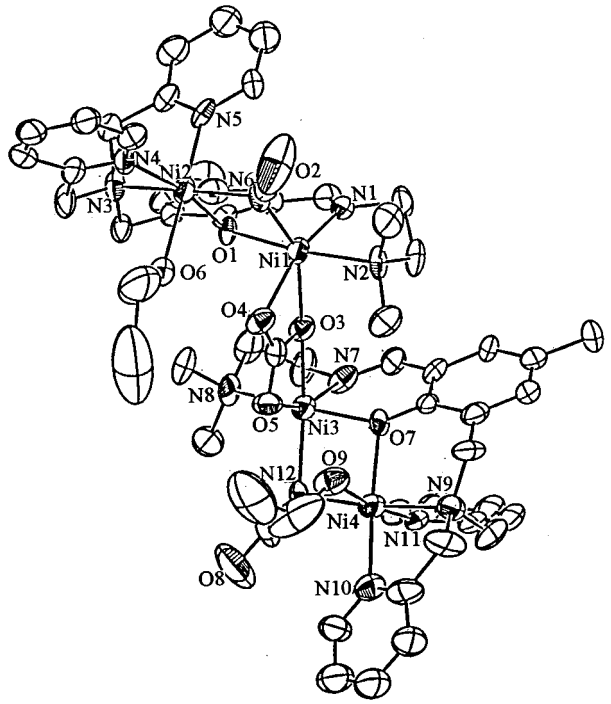

Figure 4. ORTEP view of the $[\{Ni_2(L)(NCO)(EtOH)\}_2(CO_3)]^{2+}$ part of **3′** (crystal A) with the atom numbering scheme.

to spin-allowed d−d transitions of high-spin Ni(II). A weak but sharp band is observed near 770 nm and can be assigned to a spin-forbidden transition band.

The room-temperature magnetic moments for **1** and **2** are 3.04 and 3.05 μ_B (per Ni), respectively, and decrease with decreasing temperature to 2.85 and 2.79 μ_B, respectively, at liquid nitrogen temperature. The magnetic behavior observed suggests an antiferromagnetic spin-exchange within each dinuclear core. Magnetic analyses by means of the magnetic susceptibility expression for $(S_1 = 1)-(S_2 = 1)$ system based on the isotropic Heisenberg model,

$$\chi_A = (Ng^2\beta^2/kT)[5 + \exp(-4J/kT)]/[5 + 3\exp(-4J/kT) + \exp(-6J/kT)] + N\alpha$$

gave the magnetic parameters $g = 2.13$, $J = -5.0$ cm^{-1}, and $N\alpha = 200 \times 10^{-6}$ cm^3 mol^{-1} for **1** and $g = 2.15$, $J = -7.0$ cm^{-1}, and $N\alpha = 200 \times 10^{-6}$ cm^3 mol^{-1} for **2**. In contrast the magnetic moment of **3** is practically independent of temperature (3.11 μ_B at 300 K and 3.10 μ_B at 78 K) to suggest no or a very weak magnetic interaction in this case. We have observed for related dinuclear Ni(II) complexes[33] that the magnetic interaction is generally weak and varies from antiferromagnetism to ferromagnetism on introducing slight changes in the nature of the dinuclear core.

Reaction of 1−3 with Urea. Model studies for nickel-dependent urease are of current interest,[33−40] and dinickel urea-adducts have been reported as structural models.[33,39,40] However, no functional model for urease has yet been reported although a catalytic conversion of urea into ethyl carbamate by a μ-alkoxo-μ-carboxylatodinickel(II) complex was presented recently.[40] In this work we have examined the reactivity of **1−3** toward urea in ethanol and obtained the following cyanate complexes: $[Ni_2(L)(AcO)(NCS)(NCO)]$ (**1′**), $[Ni_2(L)(AcO)(NCO)(EtOH)]PF_6$ (**2′**), $[\{Ni_2(L)(NCO)(EtOH)\}_2(CO_3)](PF_6)_2$ (**3′**). The low yields of the cyanate complexes (10−15%) were probably due to the low solubility of urea in ethanol and we have noticed that prolonged heating gave improved yields of the isocyanate complexes (17−23% after heating for 24 h). The presence of NCO^- group in **1′−3′** is supported by the fact that the reaction of **1−3** with pottasium cyanate in the 1:1 stoichiometry in ethanol gave the same cyanate complexes **1′−3′** in a better yield (>45%). The contamination of ammonium ion in crude **1′−3′** was evidenced by the IR bands at 3320 and 1410

Table 5. Selected Bond Distances (Å) and Angles (deg) with Their Estimated Standard Deviations for Crystal A of $[\{Ni_2(L)(NCO)(EtOH)\}_2(CO_3)](PF_6)_2$ (**3′**)

Ni(1)−O(1)	2.06(1)	Ni(1)−O(3)	2.16(1)
Ni(1)−O(4)	2.10(1)	Ni(1)−N(1)	2.04(2)
Ni(1)−N(2)	2.18(2)	Ni(1)−N(6)	2.15(2)
Ni(2)−O(1)	2.01(1)	Ni(2)−O(6)	2.13(1)
Ni(2)−N(3)	2.12(1)	Ni(2)−N(4)	2.07(2)
Ni(2)−N(5)	2.08(2)	Ni(2)−N(6)	2.11(2)
Ni(3)−O(3)	2.14(1)	Ni(3)−O(5)	2.10(2)
Ni(3)−O(7)	2.06(1)	Ni(3)−N(7)	2.03(2)
Ni(3)−N(8)	2.20(2)	Ni(3)−N(12)	2.13(1)
Ni(4)−O(7)	2.04(1)	Ni(4)−O(9)	2.15(2)
Ni(4)−N(9)	2.12(2)	Ni(4)−N(10)	2.06(2)
Ni(4)−N(11)	2.08(2)	Ni(4)−N(12)	2.10(2)
O(3)−C(26)	1.31(3)	O(4)−C(26)	1.27(3)
O(5)−C(26)	1.26(2)		
O(1)−Ni(1)−O(3)	90.6(4)	O(1)−Ni(1)−O(4)	93.4(5)
O(1)−Ni(1)−N(1)	88.3(6)	O(1)−Ni(1)−N(2)	171.4(6)
O(1)−Ni(1)−N(6)	79.4(6)	O(3)−Ni(1)−O(4)	62.3(6)
O(3)−Ni(1)−N(1)	93.9(6)	O(3)−Ni(1)−N(2)	91.8(5)
O(3)−Ni(1)−N(6)	151.9(6)	O(4)−Ni(1)−N(1)	156.1(6)
O(4)−Ni(1)−N(2)	95.0(6)	O(4)−Ni(1)−N(6)	91.9(6)
N(1)−Ni(1)−N(2)	83.3(7)	N(1)−Ni(1)−N(6)	111.9(6)
N(2)−Ni(1)−N(6)	101.9(7)	O(1)−Ni(2)−O(6)	83.9(5)
O(1)−Ni(2)−N(3)	90.5(6)	O(1)−Ni(2)−N(4)	167.3(5)
O(1)−Ni(2)−N(5)	92.0(6)	O(1)−Ni(2)−N(6)	81.4(6)
O(6)−Ni(2)−N(3)	92.8(5)	O(6)−Ni(2)−N(4)	87.8(6)
O(6)−Ni(2)−N(5)	173.7(7)	O(6)−Ni(2)−N(6)	89.3(5)
N(3)−Ni(2)−N(4)	80.3(7)	N(3)−Ni(2)−N(5)	82.5(6)
N(3)−Ni(2)−N(6)	171.4(7)	N(4)−Ni(2)−N(5)	95.4(6)
N(4)−Ni(2)−N(6)	108.2(7)	N(5)−Ni(2)−N(6)	94.8(6)
Ni(1)−O(1)−Ni(2)	102.0(6)	Ni(1)−N(6)−Ni(2)	95.8(7)
O(3)−Ni(3)−O(5)	61.9(5)	O(3)−Ni(3)−O(7)	91.1(4)
O(3)−Ni(3)−N(7)	95.6(6)	O(3)−Ni(3)−N(8)	92.0(5)
O(3)−Ni(3)−N(12)	151.9(7)	O(5)−Ni(3)−O(7)	92.0(5)
O(5)−Ni(3)−N(7)	157.5(6)	O(5)−Ni(3)−N(8)	97.1(6)
O(5)−Ni(3)−N(12)	91.2(6)	O(7)−Ni(3)−N(7)	87.7(6)
O(7)−Ni(3)−N(8)	170.8(7)	O(7)−Ni(3)−N(12)	81.3(5)
N(7)−Ni(3)−N(8)	83.3(7)	N(7)−Ni(3)−N(12)	110.9(7)
N(8)−Ni(3)−N(12)	99.7(6)	O(7)−Ni(4)−O(9)	82.6(5)
O(7)−Ni(4)−N(9)	90.6(5)	O(7)−Ni(4)−N(10)	167.7(7)
O(7)−Ni(4)−N(11)	90.7(6)	O(7)−Ni(4)−N(12)	82.4(5)
O(9)−Ni(4)−N(9)	94.6(6)	O(9)−Ni(4)−N(10)	88.5(7)
O(9)−Ni(4)−N(11)	172.5(5)	O(9)−Ni(4)−N(12)	89.9(7)
N(9)−Ni(4)−N(10)	81.6(7)	N(9)−Ni(4)−N(11)	82.0(7)
N(9)−Ni(4)−N(12)	171.1(7)	N(10)−Ni(4)−N(11)	97.6(7)
N(10)−Ni(4)−N(12)	106.3(7)	N(11)−Ni(4)−N(12)	92.5(7)
Ni(3)−O(7)−Ni(4)	99.6(5)	Ni(3)−N(12)−Ni(4)	95.7(6)
O(3)−C(26)−O(4)	117(2)	O(3)−C(26)−O(5)	116(2)
O(4)−C(26)−O(5)	127(2)		

(32) Downing, R. S.; Ulbach, F. L. *J. Am. Chem. Soc.* **1969**, *91*, 5977.
(33) Koga, T.; Furutachi, H.; Nakamura, H.; Fukita, Nobuo.; Ohba, M.; Takahashi, K.; Okawa, H. *Inorg. Chem.* **1998**, *37*, 989.
(34) Buchanan, R. M.; Mashuta, M. S.; Oberhausen, K. J.; Richardson, J. F. *J. Am. Chem. Soc.* **1989**, *111*, 4497.
(35) Volkmer, D.; Horstmann, A.; Griesar, K.; Hasse, W.; Krebs, B. *Inorg. Chem.* **1996**, *35*, 1132.
(36) Volkmer, D.; Hommerich, B.; Griesar, K.; Hasse, W.; Krebs, B. *Inorg. Chem.* **1996**, *35*, 3792.
(37) Hosokawa, Y.; Yamane, H.; Nakao, Y.; Matumoto, K.; Takamizawa, S.; Mori, W.; Suzuki, S. *Chem. Lett.* **1997**, 891.
(38) Watson, A. A.; Fairlie, D. P. *Inorg. Chem.* **1995**, *34*, 3087.
(39) Wages, H. E.; Taft, K. L.; Lippard, S. J. *Inorg. Chem.* **1993**, *32*, 4985.
(40) Yamaguchi, K.; Koshino, S.; Akagi, F.; Suzuki, M.; Uehara, A.; Suzuki, S. *J. Am. Chem. Soc.* **1997**, *119*, 5752.

cm^{-1}. Complexes **2′** and **3′** have an ethanol molecule in place of the methanol present in **2** and **3**. The IR spectra of **1′**−**3′** show a new vibration near 2180 cm^{-1} attributable to the cyanate ion. The electronic absorption spectra for **1′**−**3′** are similar to those of **1**−**3** and show an intense $\pi-\pi^*$ transition band at 362−366 nm and two distinct d−d bands in the visible region.

The bridging nature of the isocyanate group has been demonstrated by crystal structure analysis for **3′**. Two similar but crystallographically independent dimer-of-dimer units (A and B) exist in the lattice. An ORTEP view for the unit A is given in Figure 4, and its selected bond distances and angles are listed in Table 5.

The structure of **3′** is similar to that of **3**, except for the replacement of the hydroxy ion and the methanol ligand with the isocyanate ion and ethanol, respectively. One noticeable difference is that **3** has C_2 symmetry in the dimer structure whereas this is lacking in **3′**. In each dinuclear unit of **3′** a pair of Ni ions are bridged by the phenolic oxygen O1 and the isocyanate nitrogen N6 in the average Ni−Ni intermetallic separation of 3.14 Å. The Ni1−O1−Ni2 angle (102.0(6)°) is enlarged relative to that of **3** (99.2(3)°). The Ni2−O(ethanol) bond distance (2.13(1) Å) is short relative to the Ni2−O(methanol) bond distance in **3** (2.188(8) Å). In the isocyanato-bridged core the Ni1−N6 and Ni2−N6 bond distances are 2.15(2) and 2.11(2) Å, respectively, and the Ni1−N6−Ni2 angle is 95.8(7)°. The carbonate bridge in the dimer remains intact.

It must be emphasized that the conversion of urea into the cyanate ion is essentially stoichiometric and each complex contains only one cyanate ion per dinuclear unit. That is, **1** has two thiocyanate ions but only one of them is replaced by cyanate ion in **1′**. In the case of **2** one of two acetate groups is replaced by cyanate ion. Based on the X-ray structural result for **3′**, a dinuclear core, bridged by the phenolic oxygen of L^- and an exogenous isocyanate nitrogen atom, is also proposed for **1′** and **2′**. In these complexes the remaining acetate group may function as an additional bridge between a pair of nickel ions as judged from the small separation between the ν_{as}(COO) and ν_s(COO) vibrations modes (∼1560 and ∼1460 cm^{-1}).

A very slow dissociation of urea into ammonium and cyanate under acidic conditions is known ($NH_2CONH_2 = NH_4^+ + NCO^-$: $k = 6 \times 10^{-10}$ s^{-1} at 25 °C and pH 2).[41] The fast formation of the isocyanate complexes **1′** − **3′** under moderate pH clearly indicates that the dinuclear core plays an essential role in the conversion of urea into NCO^-. It must be noted that the conversion proceeds in absolute ethanol or acetonitrile at a comparable rate. This fact means that a hydrolytic process by a trace of water is not important in the present case. We have confirmed that the isocyanate complex **1′** is also formed in the reaction with *N*-methylurea or *N*,*N*-dimethylurea (yield ∼ 25% under conditions in Experimental), but that the complex **1** was recovered in the reaction with *N*,*N*′-dimethylurea or *N*,*N*,*N*′,*N*′-tetramethylurea. Evidently the presence of one NH_2 group is essential for the conversion of ureas into cyanate by **1**. This observation suggests that bridging of urea over the dinuclear core, through one amino nitrogen to one nickel and the carbonyl oxygen to another nickel, is a key step for the conversion. Detailed mechanistic studies remain to be performed further.

In conclusion, to the best of our knowledge this is the first recognition that urea is converted into cyanate at a dinuclear nickel core. The resulting dinickel core bridged by the phenolic oxygen and isocyanate nitrogen is highly stable when compared with other cores bearing exogenous acetate, hydroxide or isothiocyanate bridges, and this is likely to be a driving force for the conversion of urea into cyanate.

Acknowledgment. This work was supported by a Grant-in-Aid for Scientific Research (No. 09440231) from the Ministry of Education, Science and Culture, Japan. Thanks are also due to the British Council for support.

Supporting Information Available: Listing of additional analytical data (1 page). Elemental analyses and X-ray crystallographic files, in CIF format, for **1**−**3** and **1′**−**3′** are also available on the Internet only. Access and ordering information is given on any current masthead page.

IC9807689

(41) Dixon, N. E.; Gazzola, C.; Blakeley, R. L.; Zerner, R. L. *J. Am. Chem. Soc.* **1975**, *97*, 4131. Dixon, N. E.; Riddles, P. W.; Gazzola, C.; Blakeley, R. L.; Zerner, B. *Can. J. Biochem.* **1980**, *58*, 1335.